

The Effect of Partial Baffles on Natural Convection in an Inclined Rectangular Enclosure

PART I. Experimental Observations

by PAUL K.-B. CHAO*, HIROYUKI OZOE**, NOAM LIOR***, STUART W. CHURCHILL***

Abstract

Complete partitioning with honeycomb-like structures has previously been proposed to reduce heat transfer by natural convection, at the expense of direct conduction through the structure, in the thin rectangular enclosures used for solar collectors. This paper presents the results of a study of the use of partial baffles for this purpose. The heat transfer rate was measured in glycerol using heat flux meters in both the heated and cooled surfaces, and three-dimensional streaklines were photographed using tracer particles for a Rayleigh number of 2×10^4 , six baffle-configurations and a series of angles of inclination about the shorter dimension of a $2 \times 1 \times 1$ enclosure, heated and cooled on the opposing 2×1 surfaces. All of the baffle-configurations produced oblique streaklines and decreased the rate of heat transfer, but no single size or configuration was best for all inclinations. The two heat flux meters provided a measure of the net heat flux to the fluid from the Plexiglas sidewalls. A finite-difference solution for the same behavior is compared with these results in Part II of this paper.

Synopsis

This paper apparently presents the first results for the effect of a partial baffle normal to the heated and cooled surfaces of an inclined rectangular enclosure. Streaklines were photographed and heat transfer rates were measured for six baffle-configurations at a series of inclinations of the enclosure about the shorter horizontal dimension.

The internal dimensions of the test enclosure were $63.50 \times 31.75 \times 31.75$ mm, the latter being the height, giving aspect ratios of 2/1 (width/height) and 1/1 (depth/height). The vertical sides of the test cell were Plexiglas with a thick-

ness of 6.35 mm. The test cell was surrounded laterally by a vacuum chamber. Copper plates with dimensions of $254 \times 177.8 \times 19.05$ mm served as the top and bottom of the enclosure and also of the vacuum chamber. Water jackets were attached to these plates to maintain them at different, near-uniform temperatures. The periphery of both copper plates was milled out to provide space for a silver-coated, front-surface mirror. The purpose of these mirrors was to minimize radiative heat transfer between the vertical surfaces of the test enclosure and the portion of the copper plates comprising the top and bottom surfaces of the vacuum chamber.

Introduction

The work reported herein is part of a continuing investigation of natural convection in enclosures, with the primary objective of reducing heat losses across the air film in solar collectors. In recent prior work [1, 2], it was found that non-uniformities in the surface temperatures generally had an adverse effect, i.e., they increased the rate of heat transfer. The specific objective of the current work is to investigate experimentally the effect of partial baffles in suppressing convective heat transfer. Prior work on the effect of baffles on natural convection in enclosures has generally been for other applications and conditions. Complete partitions (honeycombs) of poorly conducting material, perpendicular to and extending all the way between the high and low temperature surfaces, have been proposed and utilized for solar collectors. Cane et al. [3] and Arnold et al. [4] found that existing correlations for single enclosures were applicable for the individual cells if conduction along the partitions,

and radiant interchange between the partitions and the enclosing surfaces were taken into account.

Emery [5] found that a central, vertical, partial baffle in a tall, two-dimensional enclosure, heated and cooled on the opposing vertical sides, had a negligible effect on the flow field and on the rate of heat transfer. This geometry was chosen to simulate the cooling channel of a nuclear reactor. His results are not surprising because the baffle, although extending over 90% of the height of the enclosure, was in the stagnant central core of the fluid.

Probert and Ward [6] and Janikowski et al. [7] investigated the effect of short baffles extending vertically from the insulated top and bottom walls of the same type of enclosure. The baffles were constructed of thin Perspex sheet or copper gauze. The solid baffles were found to be more effective than the porous ones, particularly when the upper baffle was placed near the cold wall and the lower baffle near the hot wall.

Several, recent investigations (e.g., [8] and [9]) are concerned with the effect of partial room-dividers on natural convection, but the boundary conditions are not relevant to this investigation. However, the following two more closely related papers have appeared since this investigation was completed. Chang et al. [10] used finite-difference calculations to determine the laminar flow patterns and rate of

* Mobil Research and Development Corporation, Paulsboro, NJ, USA

** Department of Industrial and Mechanical Engineering, Okayama University, Okayama, Japan

*** The University of Pennsylvania, Philadelphia, PA 19104, USA

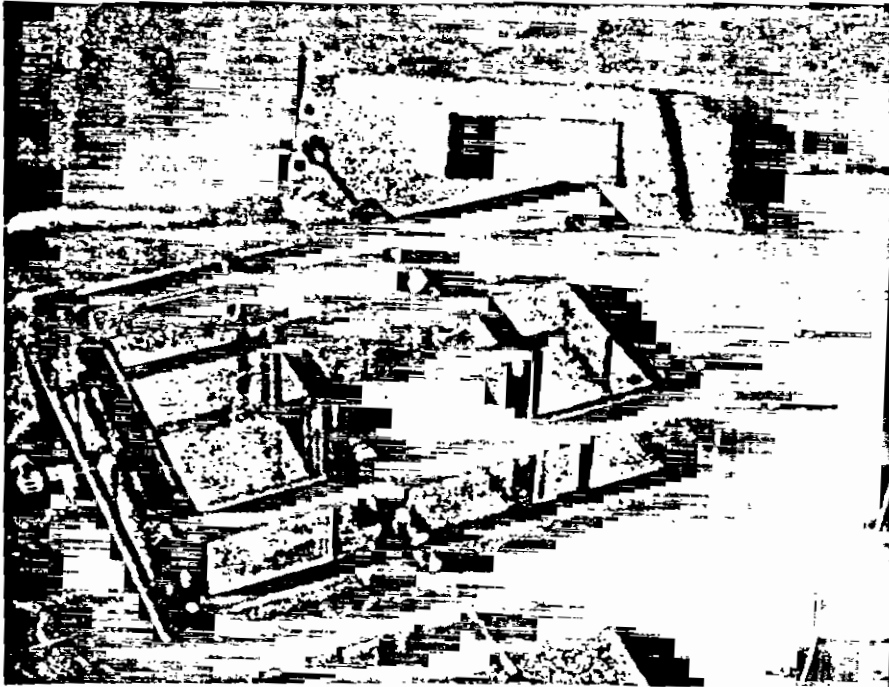


Fig. 1 Close-up of the test cavity with top plate removed

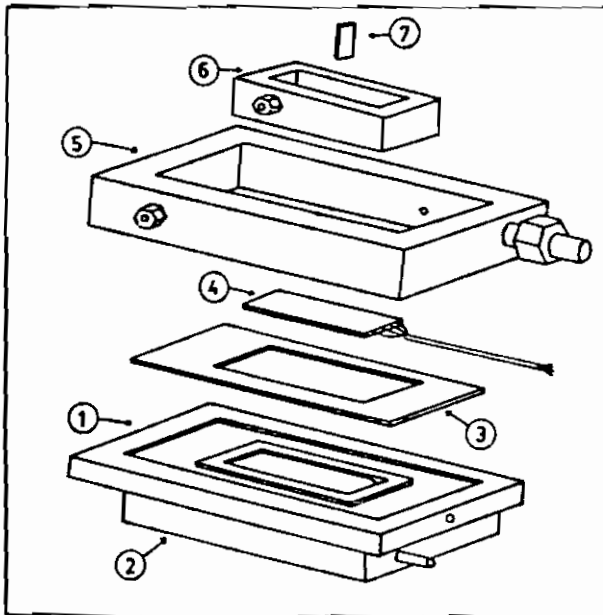


Fig. 2 Schematic drawing of the test cavity. [1] Copper plate, [2] water jacket, [3] front-surface mirror, [4] heat-flux meter, [5] vacuum chamber, [6] test cell, and [7] baffle

heat transfer in square channels, heated and cooled on the opposing vertical sides, with centrally located partitions of one-tenth width and one-quarter height attached to both the bottom and top insulated surfaces. Their calculations were for a Rayleigh number of 6.55×10^6 and a Prandtl number of 0.686, and include incrementally the effects of surface and gaseous radiation. Winters [11] carried out similar two-dimensional calculations for an enclosure with a width-to-height ratio of 8/5 and central, brass partitions in either the insulated top or bottom surface with heights of 1/4, 1/2 and 3/4, and a width of 1/16 the height of the enclosure. These calculations were for a Rayleigh number of 3.75×10^6 and a Prandtl number of 0.7. His computed

streamlines are in fair agreement with those photographed by Duxbury [12] at a slightly different Rayleigh number, using smoke injection. His photographs of the circulation patterns revealed some zones of recirculation in addition to the predicted ones, and also dissymmetry for the upper and lower locations of the partitions. This dissymmetry is probably due to heat losses, which were about 40% of that transferred. Calculations were also carried out for other aspect ratios and for partitions of different conductivities. Insofar as the Nusselt number is concerned, the partitions were found to behave as an infinite conductor, even for a conductivity as low as that of air.

The effect of partial baffles has apparently not been investigated for enclosures heated from below or inclined, or for three-dimensional convection under any conditions.

Herein, experimental rates of heat transfer and photographs of streaklines are presented for three-dimensional natural convection in an inclined $2 \times 1 \times 1$ enclosure with a single baffle of various sizes and locations. Theoretical results for this problem are presented in a companion paper [13] and compared with the experimental results.

Experimental Apparatus

The experimental apparatus, as shown in the photograph of Figure 1 and the sketch of Figure 2, consisted of a test enclosure inside a vacuum chamber. This apparatus was attached to a rotatable disk and an inclinable platform. The test cell could thus be established at any inclination up to $\pi/2$ rad and at any rotation. For inclinations from $\pi/2$ to π rad the cell was inverted. In the work reported herein, the test enclosure was inclined only about its shorter dimension. The equipment was operated in a constant-temperature room to minimize the effect of ambient changes.

The internal dimensions of the test enclosure [6] were $63.50 \times 31.75 \times 31.75$ mm, the latter being the height, giving aspect ratios of 2/1 (width/height) and 1/1 (depth/height). The vertical sides of the test cell and vacuum chamber [5] were of Plexiglas with a thickness of 6.35 mm and 9.52 mm, respectively.

Copper plates [1] with dimensions of $254 \times 177.8 \times 19.05$ mm served as the top and bottom for both the enclosure and the chamber. Water jackets [2] were attached to these plates to maintain them at different, near-uniform temperatures. Two baffles were installed in each jacket to help minimize the temperature variation over the plates. The periphery of the copper plates was milled out, as shown in Figure 2, to provide space for a 3.175 mm-thick, silver-coated, front-surface mirror [3]. The purpose of these mirrors was to minimize radiative heat exchange between the vertical surfaces of the test enclosure and the portion of the copper plates comprising the top and bottom surfaces of the vacuum chamber.

The plates were also milled out centrally, as shown, to provide for heat flux meters [4] covering the entire horizontal surface of the test enclosure. The heat flux meters were Model AB transducers made by the International Thermal Instrument Co. Their output was $\approx 13 \mu\text{V}/(\text{W}/\text{m}^2)$ and therefore did not require amplification. The heat flux meters were glued to the respective copper plates. The temperature of the fluid-contacting surface of each heat flux meter was measured with a copper-constantan thermocouple. The four lead wires from the heat flux meter and thermocouple passed under the inner and through the outer raised rings of the copper plates.

The output of the thermocouple from each meter, their difference, and the output of the two heat flux meters themselves were periodically displayed on a Keithly 160B digital multimeter and recorded on a Keithly 750 printer, using a manual thermocouple switch.

O-rings, as shown in Figure 2, were used to seal the vacuum chamber from the test enclosure and the surroundings. A pressure of 1–2 Pa was maintained in this chamber by continuous operation of the vacuum pump, and was mentioned with a Pirani gauge. At this pressure, heat transfer by thermal conduction in air is less than 1% at that of atmospheric pressure.

An infinite number of combinations of baffle widths, heights, thicknesses, locations and materials are possible. The baffles used in these experiments were cut from the transparent plastic sheets used with overhead projectors. They had a thickness of 1.5 mm and were attached with small strips of two-sided Scotch-brand adhesive tape. Seven configurations were used as shown in the inset of Figure 5.

The experiments are intended primarily to simulate natural convection in air. However, prior work has shown that natural convection in air is approximately the same in dimensionless terms as for high-Prandtl number fluids. Therefore, 99% glycerol (Sigma Chemical Co. No. G 77-57) was chosen as the working fluid because of its greater density, thermal conductivity and viscosity. The greater thermal conductivity and density minimize the relative effects of conduction through and along the side walls. The greater viscosity and density provide a larger time-constant and reduce the sensitivity to external perturbations. The greater density also impedes the diffusion of the suspended particles used for visualization. The properties of glycerol were taken from Newman [14].

The glycerol was introduced into the test enclosure through a hypodermic needle, passing horizontally through compression fittings with rubber inserts in the Plexiglas walls as indicated in Figure 2. The displaced air escaped through a second needle. Once the cavity was filled, one needle was closed and the other left open to allow for thermal expansion and contraction of the glycerol.

For visualization of the flow, a suspension of aluminium flakes in glycerol was injected at various depths by means of a smaller hypodermic needle passing through the glycerol injection needles. The aluminium flakes align with the shear planes of the flow, promoting coherent reflection of the incident illumination so that clear pictures of the streaklines can be obtained.

Photographs of the aluminium flakes were taken with ASA 400, black and white film, using a 35 mm Pentax camera with an extension tube. A narrow strip of light from a 35 mm projector was used to illuminate selected regions of the fluid.

Experimental Procedure

The two heat flux meters were first calibrated in the two possible juxtapositions by comparison with the theoretical heat flux for pure thermal conduction (with the higher-temperature plate A on top). The results are shown in Figure 3. Because of the lower scatter and the smaller correction ($\sim 2\%$), heat flux meter No. 2 on the higher-temperature surface was used for the primary results presented herein.

The water baths and jackets were operated to produce temperatures of $27.75 \pm 0.05^\circ\text{C}$ and $31.55 \pm 0.05^\circ\text{C}$ on the fluid-contacting surfaces of the heat flux meters. These temperatures correspond to the upper and lower surfaces, respectively, in their initial uninclined position. This temperature difference produces a Rayleigh number of $\sim 2 \times 10^4$.

Twelve to twenty-four hours were required to establish a steady state at each inclination. The flow pattern was observed at six inclinations, using fresh glycerol for each run. After the steady state was attained, aluminium flakes were introduced. Forty more minutes were required for the flakes to establish good streakline patterns. By 90 minutes the aluminium flakes were too dispersed to reveal distinct streaklines.

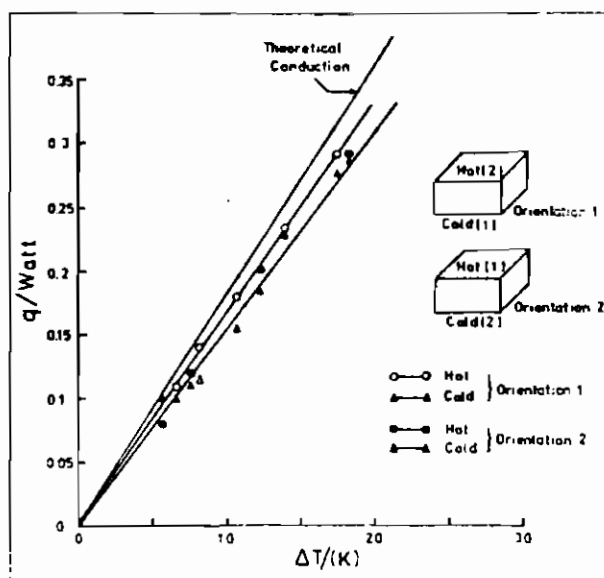


Fig. 3 Calibration of the two heat flux meters in two horizontal orientations

Heat Flux Measurements

The Nusselt number is defined as the ratio of heat transferred by thermal conduction alone. For these experiments

$$Nu = \frac{q + \Delta q}{q_c} \quad (1)$$

where

q_c = theoretical heat flux due to thermal conduction, W

q = heat flux from meter, W

Δq = correction factor for heat flux meter, as determined from Figure 3, W

Figure 4 is a plot of Nu as determined at the surfaces for no baffle. The value determined at the lower-temperature plate has a much higher maximum at no inclination than at $\pi/3$ rad. The reason for this anomaly became evident when the streakline experiments were conducted. For the horizontal orientation, the stable circulation pattern consists of two roll-cells with their axes parallel to the shorter horizontal dimension. Theoretically, for a fluid that conforms to the Boussinesq approximations, the probability is equal for circulation in either direction (upward or downward in the central plane and conversely at the ends). In these experiments the circulation was always upward near the center of the 2×1 plane and downward near the distant walls, and indeed could not be induced to circulate steadily in the opposite direction. This preferred mode of circulation, as opposed to downward flow in the center, is presumably caused by a slightly greater heat flux density near the midplane than at one end owing to the presence of the lead wires at that end.

Since the Plexiglas endwalls have a higher thermal conductivity than the fluid, a net amount of energy enters the fluid from the vertical walls and a greater total heat flux is transferred from the fluid to the cooled, horizontal plate than enters from the heated horizontal plate. If the fluid circulated downward at the center and upward along the endwalls, energy would be transferred from the passing heated fluid, and the heat flux from the fluid to the cooled plate would be less than that from the heated plate to the fluid.

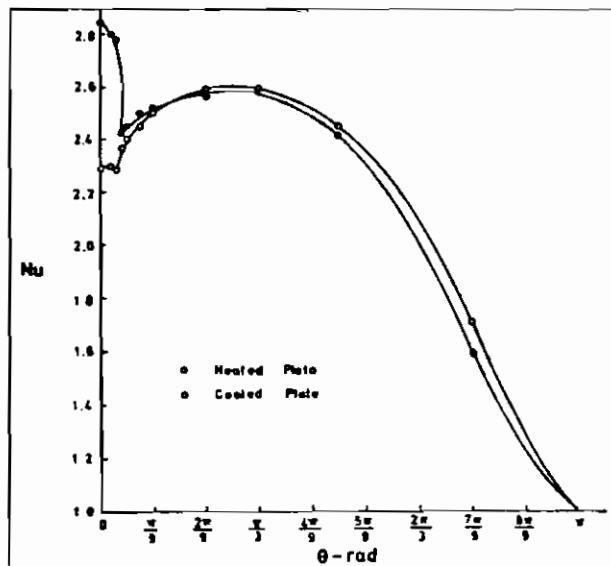


Fig. 4 Measured Nusselt numbers on heated and cooled plates for an un baffled enclosure

For inclinations just beyond that for the minimum in the heat flux, the fluid moves up along the inclined heated surface as a single roll-cell, and the elevated endwall has a lower temperature and the unelevated endwall a higher temperature than the passing fluid, thus minimizing the net transfer from the endwalls to the fluid. As a consequence, the Nusselt numbers for the heated and cooled surfaces differ insignificantly for inclinations greater than $\pi/9$ rad. The Nusselt number determined from the heated plate is believed to be more representative of the idealized case of non-conducting sidewalls than that from the cooled plate or their average, and is considered exclusively hereafter. These values from the heated plate are also in better agreement with prior measured and computed values for the limiting case of no baffles.

The Nusselt numbers determined from the heat flux meter on the higher-temperature plate are plotted in Figure 5 for the indicated configurations of the baffle. A minimum in the rate of heat transfer occurs between $5\pi/180$ and $10\pi/180$ rad and a maximum between $40\pi/180$ and $60\pi/180$ rad for all configurations.

Case 1, for no baffle, shows the highest rate of heat transfer at all angles of inclination. The one-quarter baffle, Case 2, produces a significant reduction in the Nusselt number at all inclinations, but the least of any of the baffled configurations for inclinations greater than $4\pi/9$. Comparison of Cases 2, 3, and 6 indicates that the extension of the baffle reduces Nu for all inclinations beyond $20\pi/180$ rad. For lesser inclinations the optimal baffle-width is inclination-dependent.

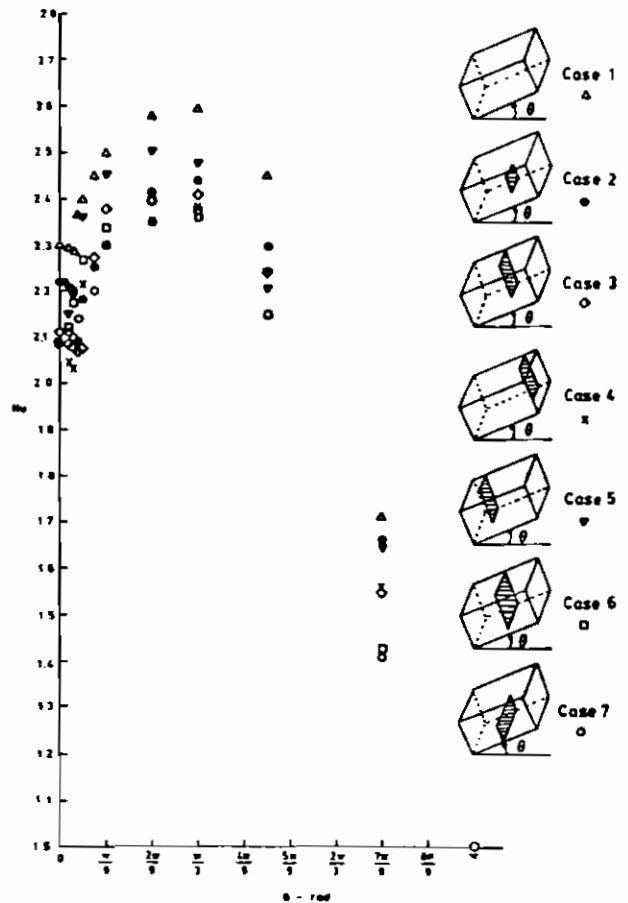


Fig. 5 Experimental Nusselt numbers at various angles of inclination and baffle-configurations

Location of the baffle near the elevated end, as in Case 4, reduces the rate of heat transfer, whereas location near the unelevated end, as in Case 5, increases the rate, relative to the central location of Case 3.

Case 7, with a baffle of half-height, completely across the enclosure, generally reduces the Nusselt number more than the other configurations, for all inclinations greater than $15\pi/180$ rad.

It is concluded that the heat flux can be reduced by the installation of a baffle, and that the optimal size and location of the baffle depend on the angle of inclination.

Photographs of Streaklines

Figures 6–38 are photographs of streaklines for the seven configurations listed above. The viewing angles are indicated at the top and the specific fields of illumination below the photographs. The apparatus had to be cleaned out after each run. Hence, a more limited number of angles of inclination were investigated than for the heat transfer rate. Twenty-four hours was allowed for the establishment of a steady state before injection of the aluminium tracers. Because of the copper plates, photographs were possible only from the four sides. Therefore, a sketch was constructed of the presumed top view of the streaklines.

Case 1

Figures 6–8 show streaklines for no baffle. For no inclination, as shown in Figure 6, there are two roll-cells, symmetrical about the shorter vertical midplane, each composed of two half-cells, symmetrical about the longer vertical midplane. The axes of these cells are parallel to the shorter horizontal dimension, with upflow in the midplane, as sketched.

For an inclination of $4\pi/180$ rad, as shown in Figure 7, the roll-cell moving up the heated surface increases at the expense of the other. At an inclination of $8\pi/180$ rad, as shown in Figure 8, the weaker cell has disappeared, and the circulation consists of a single 2×1 roll-cell moving up along the inclined heated surface and down along the cooled surface.

Case 2

Figure 9 shows the motion for the quarter-baffle with no inclination. The motion is very similar to that of Figure 6 for no baffle. However, for $4\pi/180$ rad of inclination, as shown in Figure 10, the axis of the roll-cell at the inclined end has become quite oblique and the upper roll-cell extends into the lower half of the enclosure. At $8\pi/180$ rad of inclination, as shown in Figure 11, both of the rear half-cells are oblique to the shorter horizontal dimension, and the frontal half-cells appear to have coalesced. At $20\pi/180$, $60\pi/180$ and $90\pi/180$ rad, as shown in Figures 12–14, the single frontal roll-cell is similar to that of Case 1 for large inclinations, whereas the rear half-cells have also coalesced to a single roll-cell with the form of a continuous typewriter ribbon.

Case 3

This configuration was photographed in Japan with the experimental setup described by Ozoe, et al. [15]. It should be noted that the elevation in these photographs is on the left instead of on the right, also that the circulation is downward at the center. Streaklines and sketches for inclinations of 0, $5\pi/180$ and $10\pi/180$ rad are shown in Figure 15 and $20\pi/180$, $45\pi/180$ and $90\pi/180$ rad in Figure 16. For no inclination the circulation is seen to be similar to that of Figure 6. At $5\pi/180$ rad the roll-cell at the elevated end is quite oblique and the one at the other end has rotated $\pi/2$ rad. By $10\pi/180$ rad the elevated roll-cell has wrapped around the baffle. For inclinations of $45\pi/180$ and greater the axes of the two roll-cells on the baffled side of the enclosure and the coupled roll-cell on the unbaffled side have become nearly parallel to the shorter horizontal dimension.

Case 4

For the baffle location near the elevated end, as shown in Figures 17–22, the circulation pattern is more complicated. Even for no inclination the axis of the rear half-cell at the elevated end is roughly parallel to the longer horizontal dimension, while the associated frontal half-cell is in front and on the downslope side of the baffle, but with its axis nearly parallel to the shorter horizontal dimension. At inclinations of $4\pi/180$ and $8\pi/180$ rad the axis of the upslope half-cells become oblique. At $20\pi/180$ rad the two upslope half-cells appear to have coalesced to a single roll-cell with its axis in the longer horizontal dimension, and the frontal half-cell on the downslope side has expanded to 2×1 roll-cell in front of the baffle. At $60\pi/180$ rad the roll-cell on the upslope side of the baffle has rotated $\pi/2$ rad so that all three axes are parallel to the shorter horizontal dimension. This pattern persists at $90\pi/180$ rad.

Case 5

For the baffle location near the unelevated end of the enclosure the circulation is again very complicated, as illustrated in Figures 23–28. For no inclination the roll-cells are remarkably oblique, as best indicated by the sketch of the presumed downward view. At $4\pi/180$ rad the pattern is further developing, but at $8\pi/180$ rad has become similar to the mirror image of Figure 20. By $20\pi/180$ rad the roll-cell on the downslope side of the baffle has rotated $\pi/2$ rad, and at an inclination of $90\pi/180$ rad the roll-cells in front of and below the baffle appear to be coalescing.

Case 6

The circulation pattern for the three-quarter baffle is shown in Figures 29–34. For no inclination the circulation is symmetrical about the baffle but the rear half-cells have approximately the length of the baffles. For an inclination of $4\pi/180$ rad the half-cells on the downslope side have become stronger and those on the upslope side oblique. This pattern persists at $10\pi/180$ rad, but at $20\pi/180$ rad the single frontal cell has the configuration of a continuous typewriter ribbon, as previously noted in Figures 12–24, and this pattern persists at $90\pi/180$ rad.

Case 7

The baffle of full-width but half-height results in a somewhat different pattern of circulation on elevation, as might be expected. The pattern for no inclination is similar to that of Figure 6 and hence is not shown. The photographs for $6\pi/180$, $10\pi/180$, $40\pi/180$ and $90\pi/180$ rad of inclination

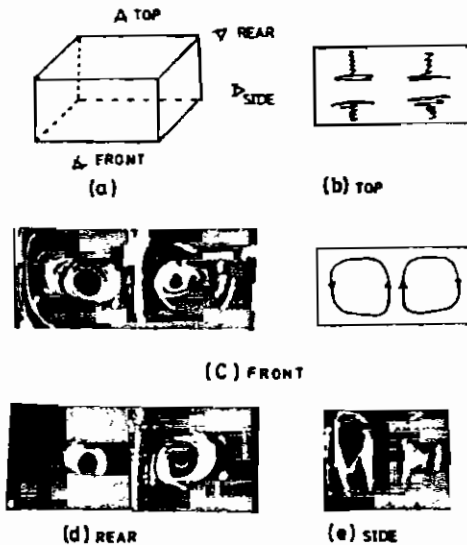


Fig. 6 Streaklines for Case 1 (no baffle) with no inclination

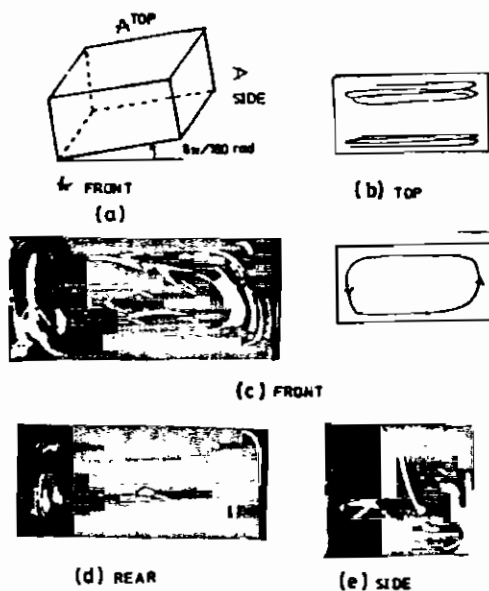


Fig. 8 Streaklines for Case 1 (no baffle) with $8\pi/180$ rad of inclination

are, however, shown in Figures 35–38. At an inclination of $6\pi/180$ rad both roll-cells have become highly oblique. At $10\pi/180$ rad the two rear and the two frontal half-cells appear to be coalescing, and at $40\pi/180$ rad and $90\pi/180$ rad a single continuous typewriter-ribbon pattern is very evident with symmetrical frontal and rear half-cells.

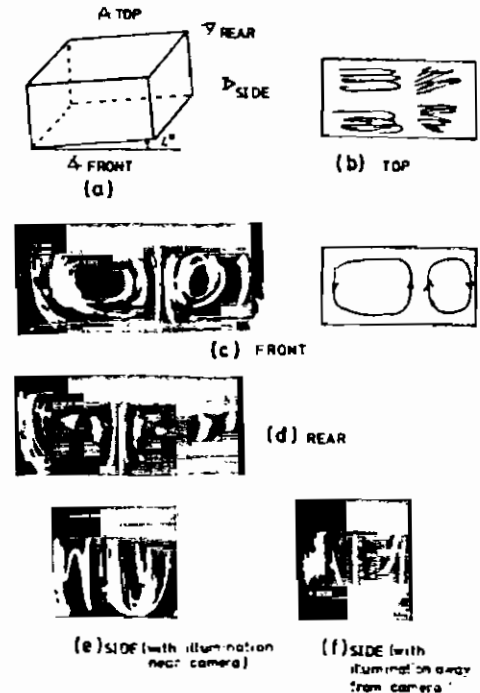


Fig. 7 Streaklines for Case 1 (no baffle) with $4\pi/180$ rad of inclination

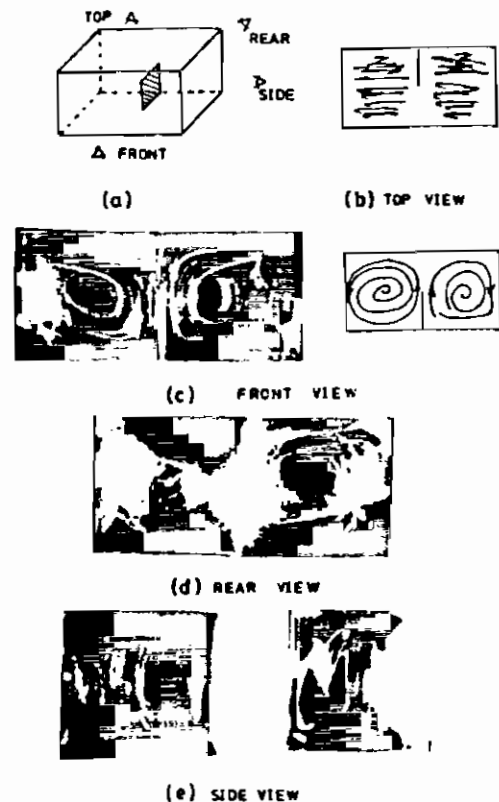


Fig. 9 Streaklines for Case 2 with no inclination

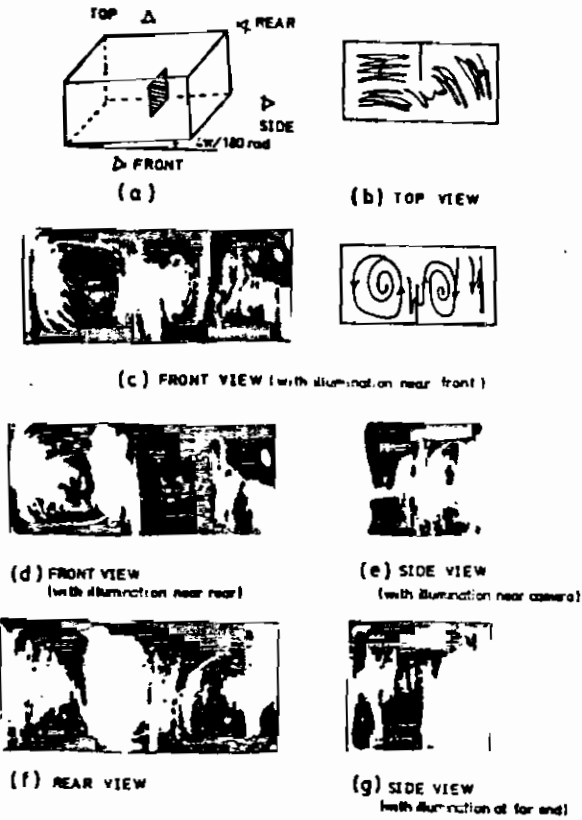


Fig. 10 Streaklines for Case 2 with $4\pi/180$ rad of inclination

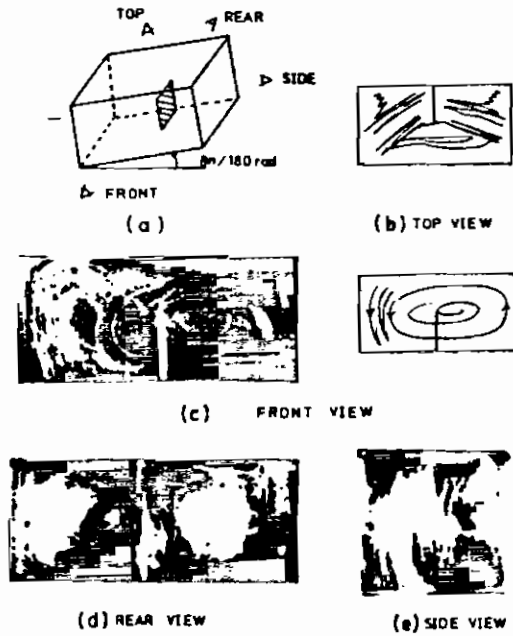


Fig. 11 Streaklines for Case 2 with $8\pi/180$ rad of inclination

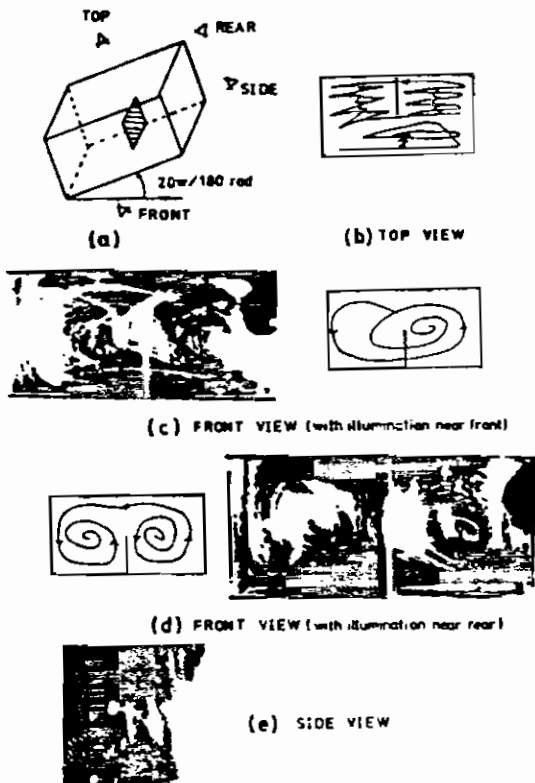


Fig. 12 Streaklines for Case 2 with $20\pi/180$ rad of inclination

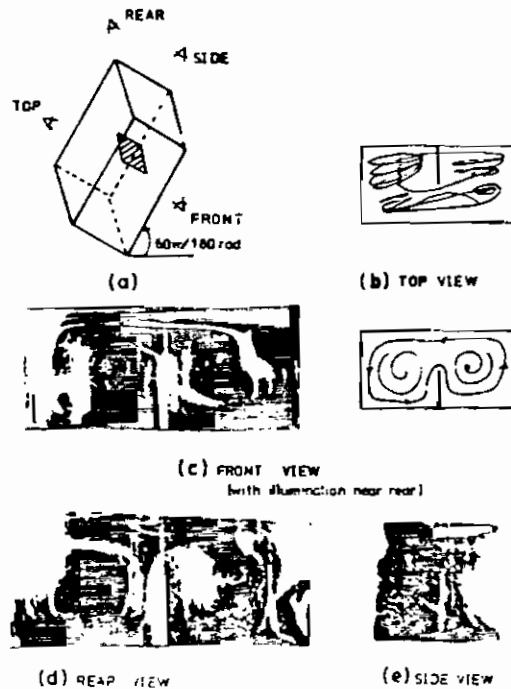


Fig. 13 Streaklines for Case 2 with $60\pi/180$ rad of inclination

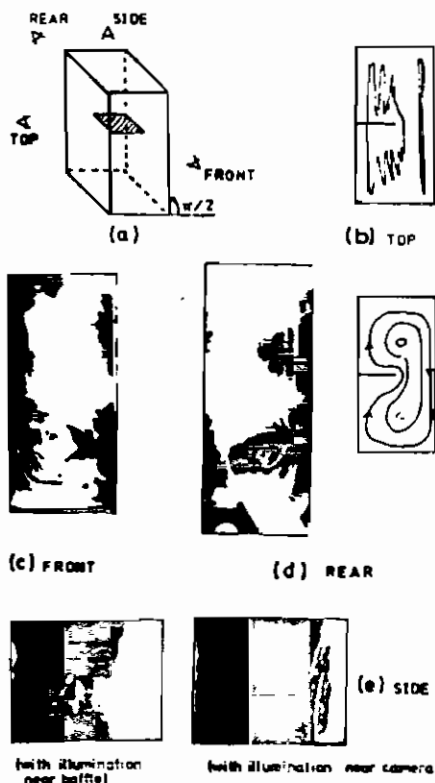


Fig. 14 Streaklines for Case 2 with $\pi/2$ rad of inclination

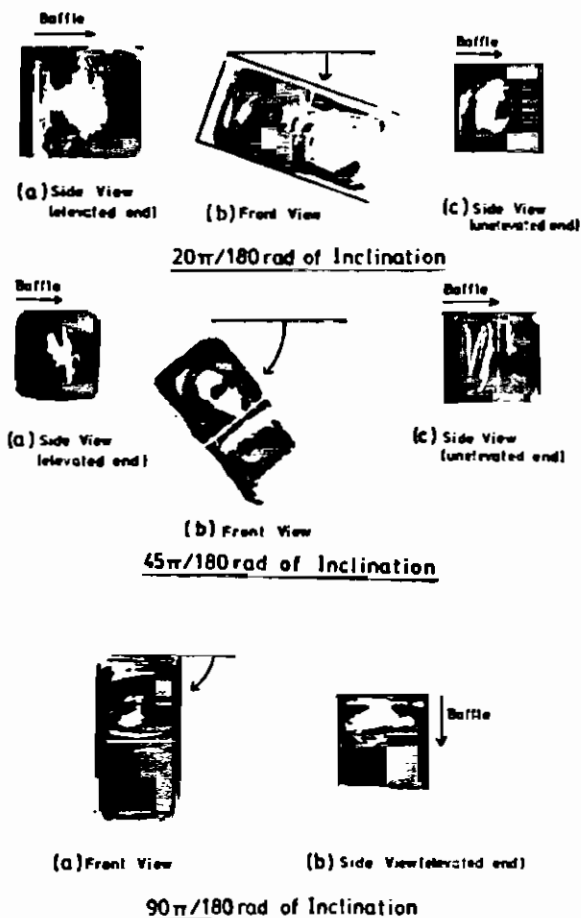


Fig. 16 Streaklines for Case 3 with $20\pi/180$, $45\pi/180$ and $90\pi/180$ rad of inclination

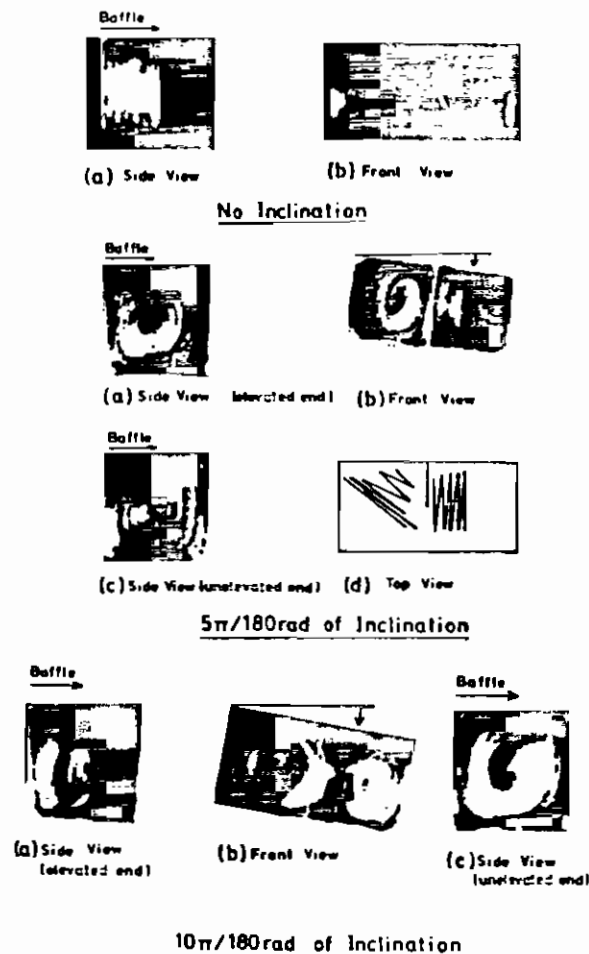


Fig. 15 Streaklines for Case 3 with 0 , $5\pi/180$ and $10\pi/180$ rad of inclination

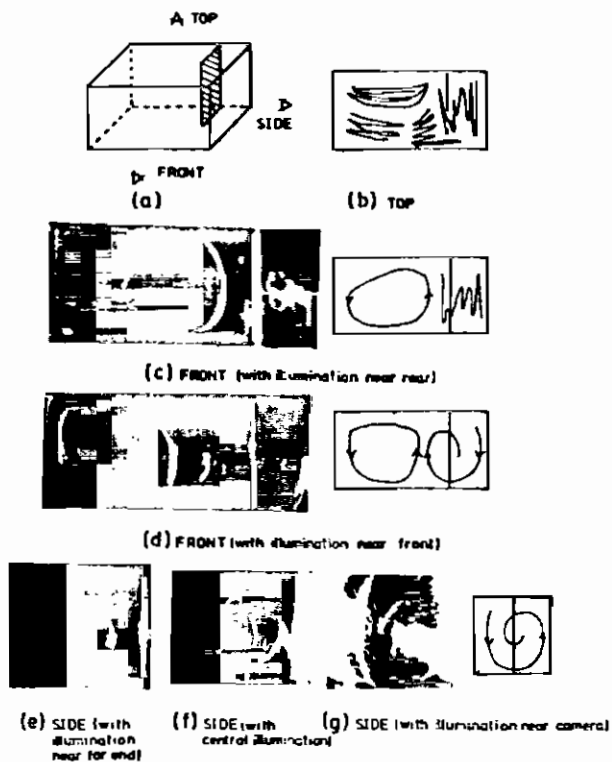


Fig. 17 Streaklines for Case 4 with no inclination

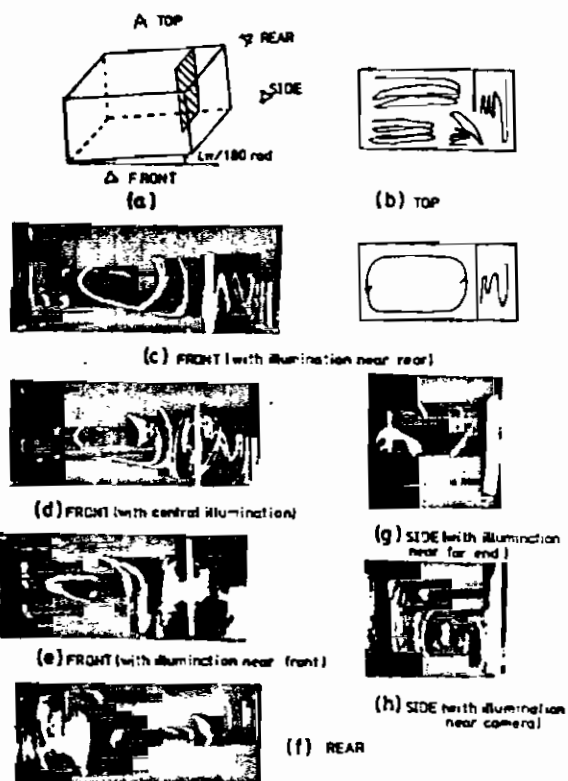


Fig. 18 Streaklines for Case 4 with $4\pi/180$ rad of inclination

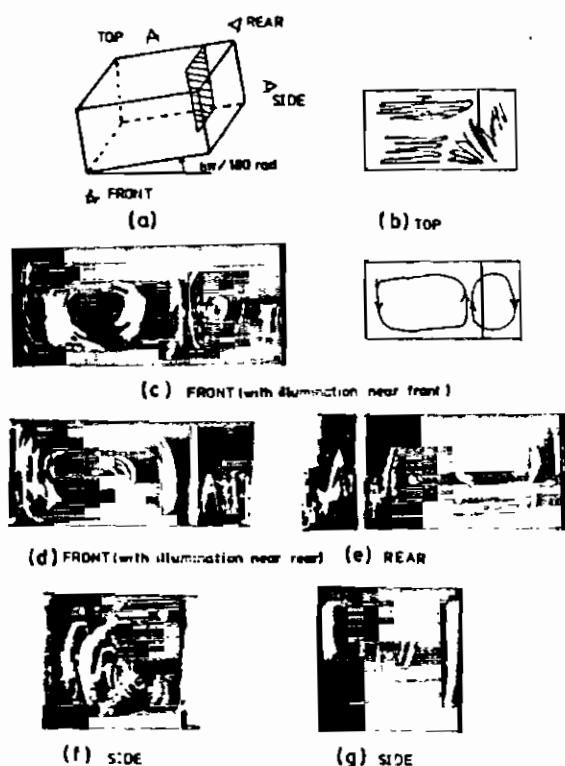


Fig. 19 Streaklines for Case 4 with $8\pi/180$ rad of inclination

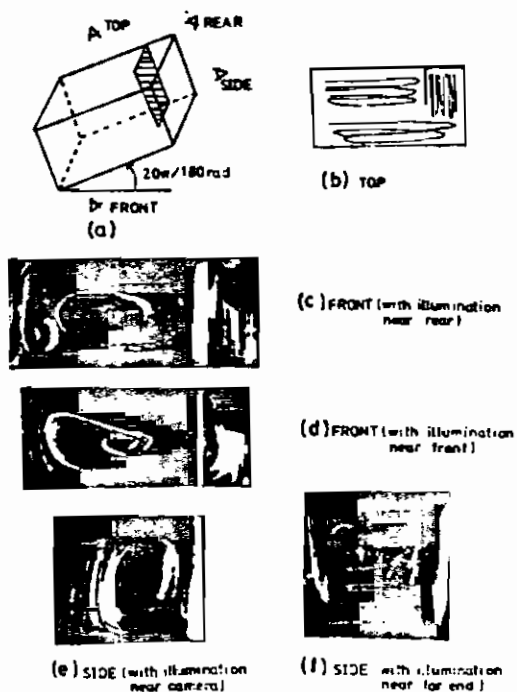


Fig. 20 Streaklines for Case 4 with $20\pi/180$ rad of inclination

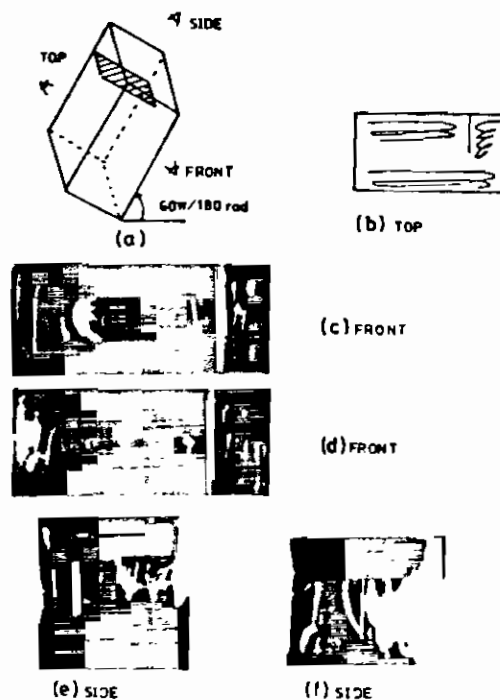


Fig. 21 Streaklines for Case 4 with $60\pi/180$ rad of inclination

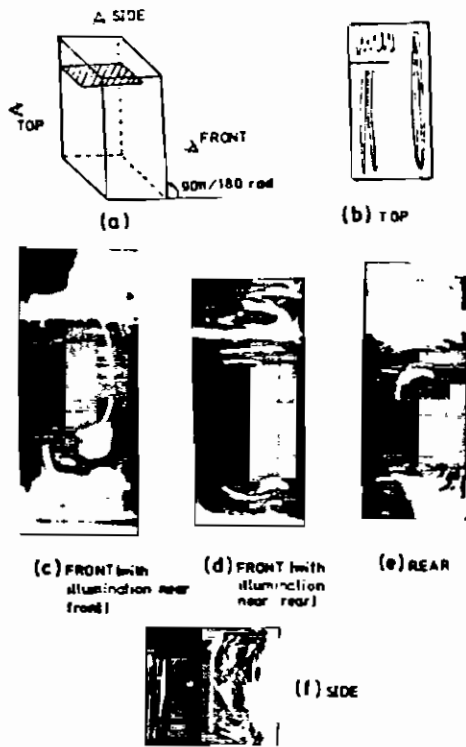


Fig. 22 Streaklines for Case 4 with $90\pi/180$ rad of inclination

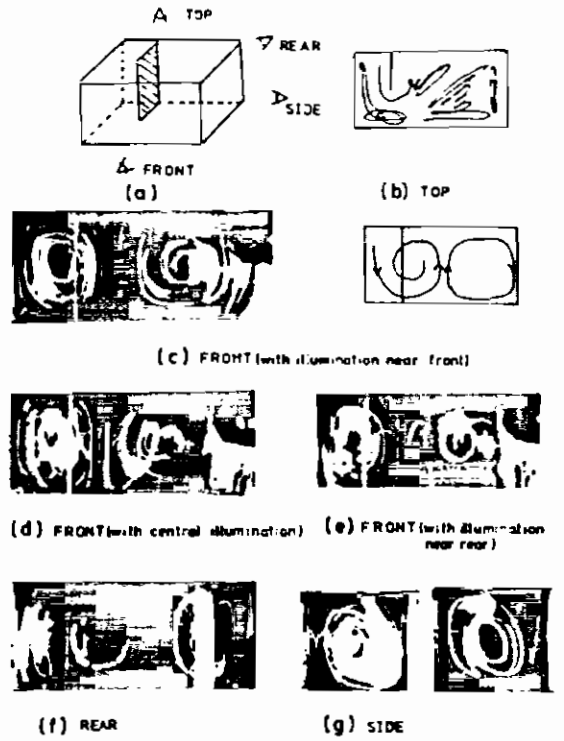


Fig. 23 Streaklines for Case 5 with no inclination

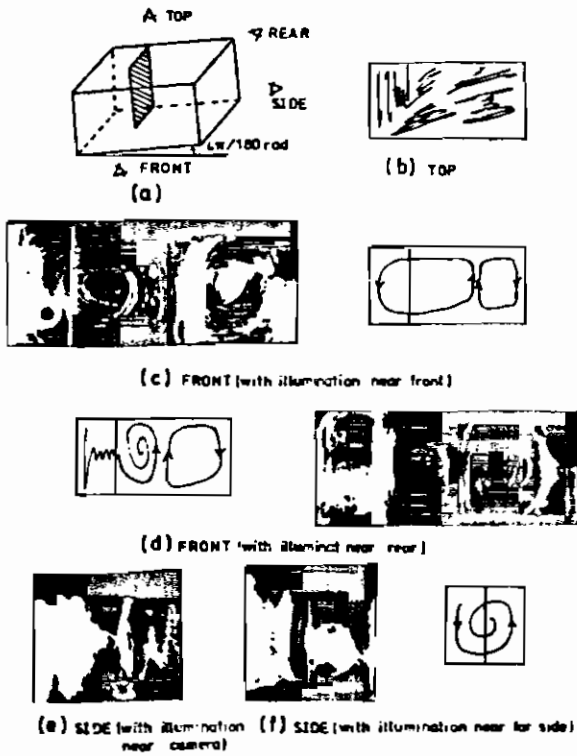


Fig. 24 Streaklines for Case 5 with $4\pi/180$ rad of inclination

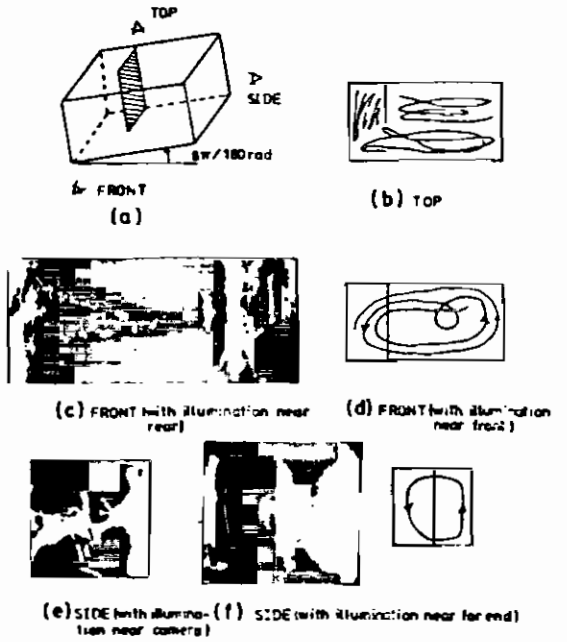


Fig. 25 Streaklines for Case 5 with $8\pi/180$ rad of inclination

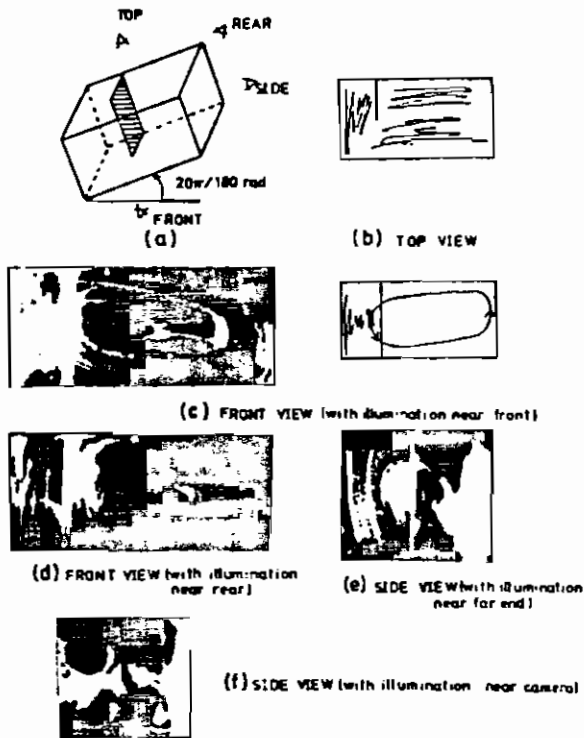


Fig. 26 Streaklines for Case 5 with $20\pi/180$ rad of inclination

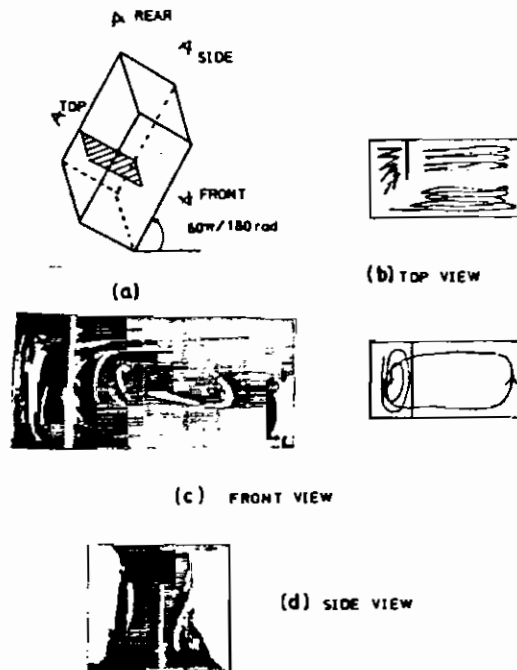


Fig. 27 Streaklines for Case 5 with $60\pi/180$ rad of inclination

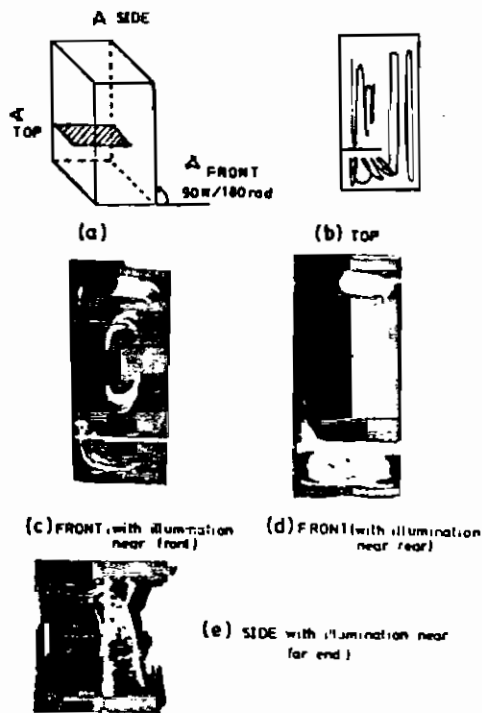


Fig. 28 Streaklines for Case 5 with $90\pi/180$ rad of inclination

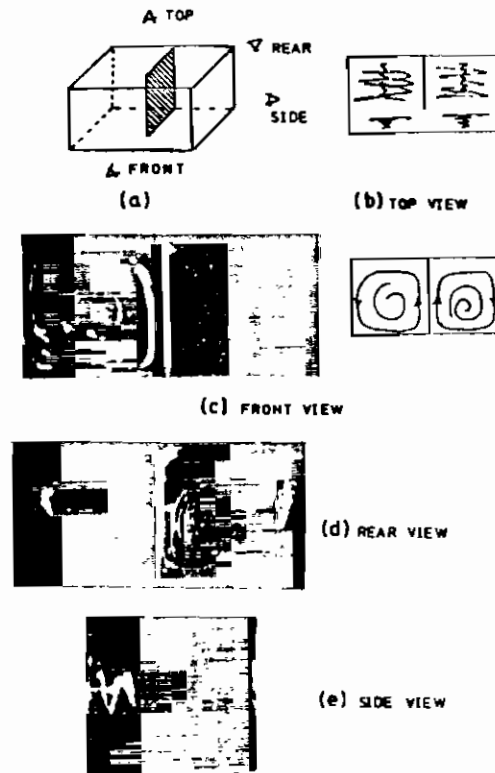


Fig. 29 Streaklines for Case 6 with no inclination

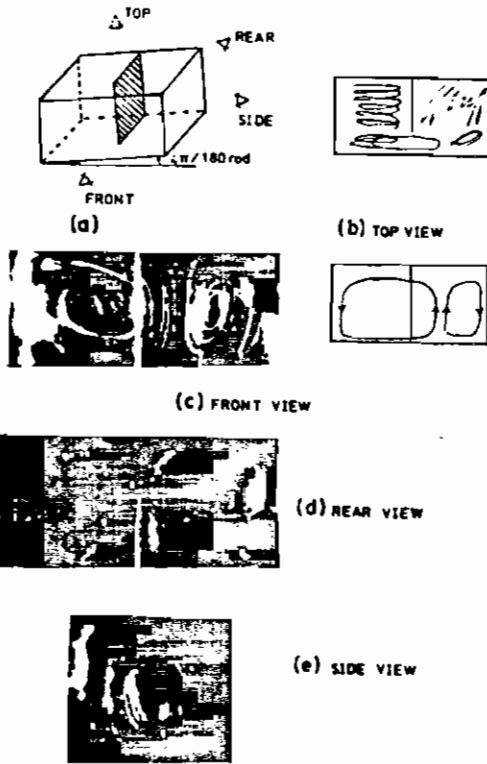


Fig. 30 Streaklines for Case 6 with $4\pi/180$ rad of inclination

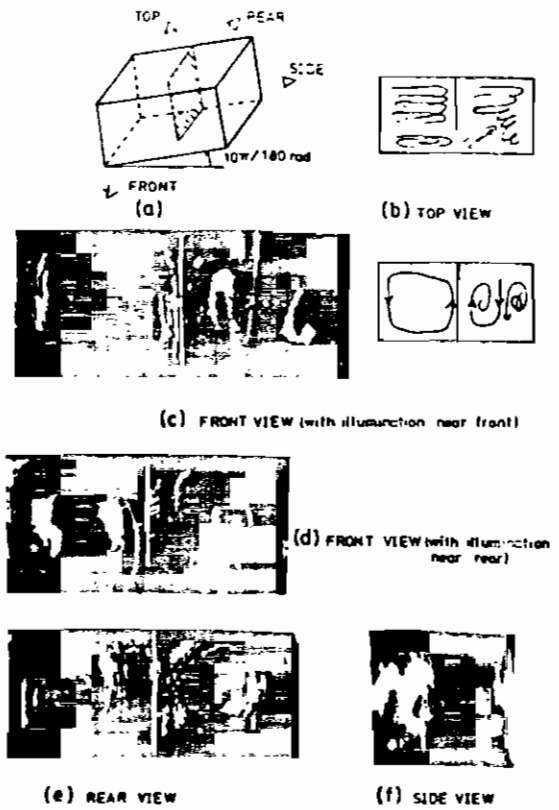


Fig. 31 Streaklines for Case 6 with $10\pi/180$ rad of inclination

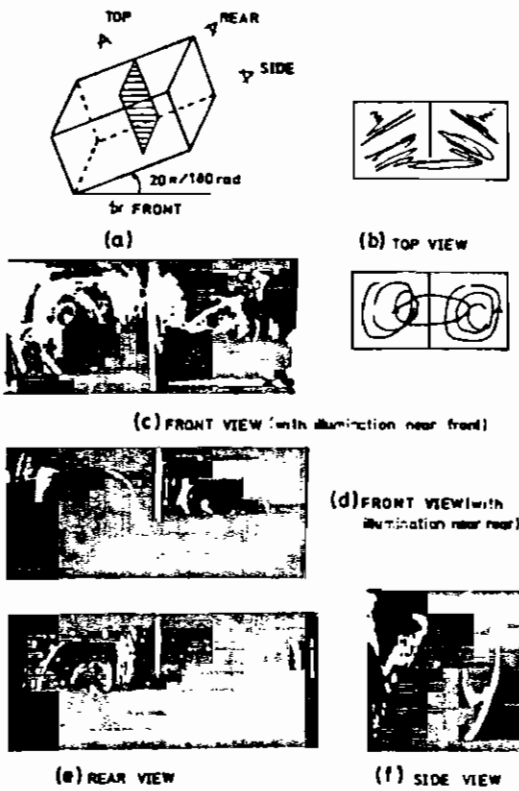


Fig. 32 Streaklines for Case 6 with $20\pi/180$ rad of inclination

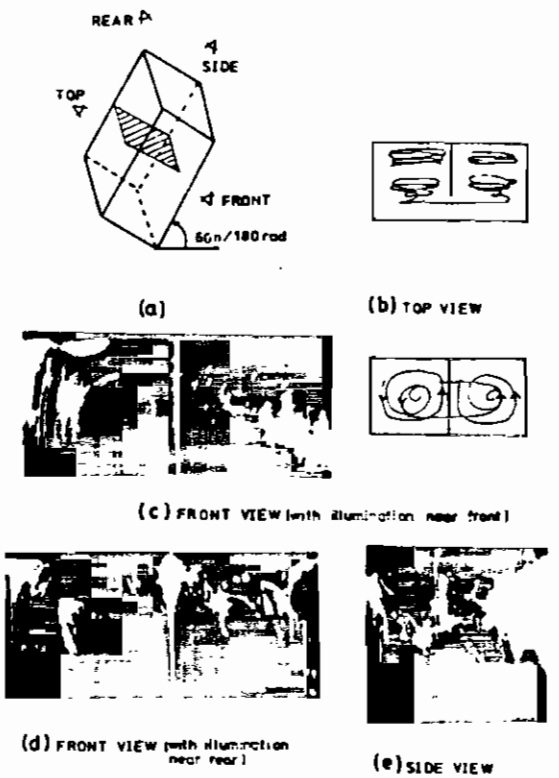


Fig. 33 Streaklines for Case 6 with $60\pi/180$ rad of inclination

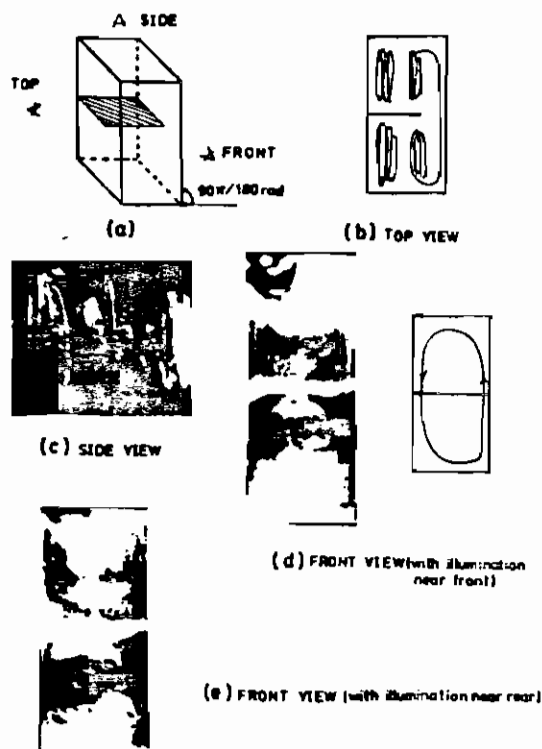


Fig. 34 Streaklines for Case 6 with $90\pi/180$ rad of inclination

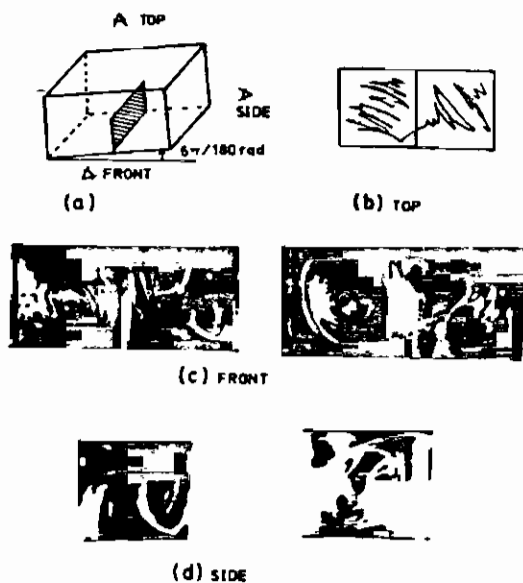


Fig. 35 Streaklines for Case 7 with $6\pi/180$ rad of inclination

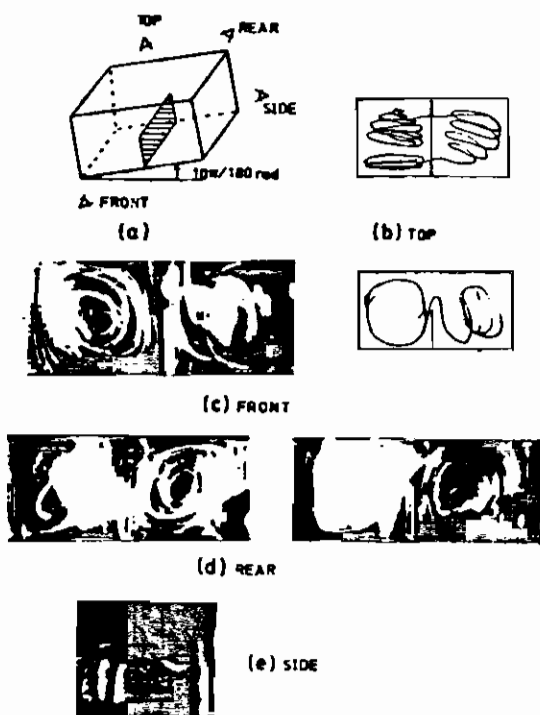


Fig. 36 Streaklines for Case 7 with $10\pi/180$ rad of inclination

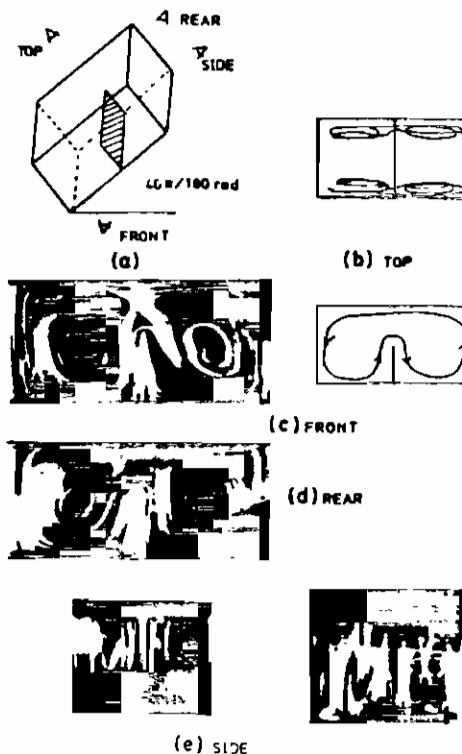


Fig. 37 Streaklines for Case 7 with $40\pi/180$ rad of inclination

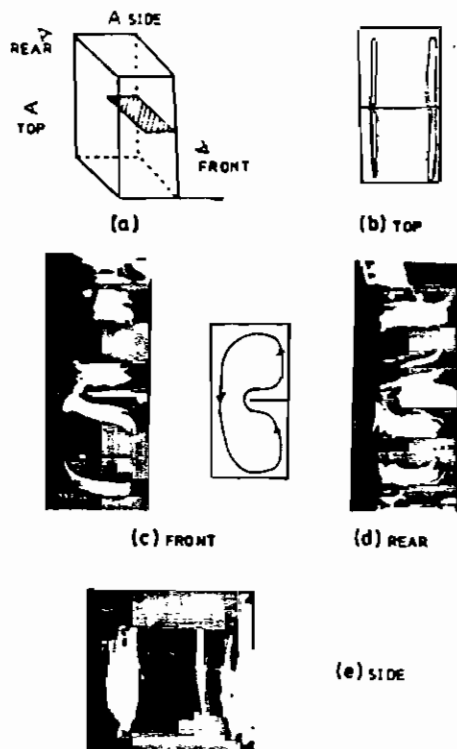


Fig. 38 Streaklines for Case 7 with $90\pi/180$ rad of inclination

Interpretation and Conclusions

The photographs of tracer particles reveal complex but highly structured patterns of circulation due to natural convection in inclined, partially baffled, rectangular enclosures. The rate of heat transfer across the enclosure is shown to be related closely to these flow patterns.

For a $2 \times 1 \times 1$ rectangular enclosure, with heating and cooling on the opposing 2×1 surfaces, the circulation for heating from below consists of two symmetrical roll-cells with their axes parallel to the shorter horizontal dimension. These roll-cells each consist of two symmetrical half roll-cells. As the enclosure is inclined about the lesser horizontal dimension as an axis, the roll-cell whose motion is upward along the inclined surface grows in size and strength at the expense of the other roll-cell, which is opposed by the buoyant force and eventually vanishes. In this work the initial roll-cells circulated upward at the center and down along the endwalls owing to the slight non-isothermality of the surfaces. As a consequence, the upper roll-cell diminished and vanished.

The average rate of heat transfer across the enclosure at first decreases with inclination, then goes through a minimum and increases to a maximum higher than the value for no inclination. This maximum is attained when the diagonal plane of the enclosure is vertical. Finally, the rate of heat transfer decreases to zero for an inclination of π rad, corresponding to heating from above, with no circulation. The above description of the circulation and heat transfer is in conformity with prior observations.

All of the baffle sizes and locations which were tested in this investigation produced oblique roll-cells, particularly for low angles of inclination. As the inclination of the heated surface was increased to $\pi/2$ rad the axes of circulation again became parallel to the lesser horizontal dimension.

All of the baffle-configurations of this investigation reduced the overall rate of heat transfer at all angles of inclination, presumably because of the oblique patterns of flow and the related decrease in the rate of circulation.

No one baffle-configuration was best for all angles of inclination. For inclinations from $2\pi/9$ to π rad increasing the height and/or width of the baffle produced a monotonic decrease in the rate of heat transfer. Location of a baffle of half-width and full-height near the elevated end of the enclosure reduced the rate of heat transfer relative to central or lower locations. A baffle of half-height and full-width produced the greatest reduction in the rate of heat transfer for all inclinations greater than $\pi/9$ rad.

The maximum reduction in the rate of heat transfer which was achieved with these baffles varied from about 10% at no inclination up to about 20% at $7\pi/9$ rad, and of course, down to zero at π rad. It is probable that comparable reductions can be achieved in enclosures of greater aspect ratios.

The effect of the thermal conductivity and finite thickness of the Plexiglas endwalls on the respective heat fluxes from the heated plate to the fluid and to the cooled plate from the fluid was fortuitously revealed by the use of heat flux meters in both surfaces. For the case of heating from below, the cooled fluid leaving the cold plate picks up heat while flowing down past the endwalls, which have a mean temperature equal to the average of the hot- and cold-plate temperatures. The consequence is that the heat transferred to the cold plate is equal to that leaving the hot plate plus this increment. For the experimental apparatus and conditions of this study, the heat flux to the cold plate was about 25% greater than that leaving the hot plate. If the endwalls were perfect insulators or vanishingly thin, this increment would approach zero.

As the enclosure is inclined, the roll-cell at the elevated end decreases in size and rate of circulation, and eventually disappears. Thereafter, the flow pattern consists of a single roll-cell circulating upward at the elevated end and downward at the other, the net heat transfer between the endwalls and the fluid approaches zero, and nearly the same heat flux passes between the fluid and the hot and cold plates.

Under idealized conditions the opposite direction of circulation is equally probable for heating from below, i.e., downward in the center and upward along both endwalls. A net heat flux would then occur from the fluid to the colder endwalls, and about 25% less heat exchange would take place from the fluid to the cold plate than from the hot plate to the fluid.

The consistently observed direction of circulation for no inclination, i.e., upward near the center, is presumably an artifact of a slight non-isothermality in the heated and cooled surfaces. This sensitivity of the circulation pattern to minor perturbations in the boundary conditions should always be a consideration in interpreting experiments for laminar natural convection. The minor details of the circulation patterns observed in this investigation may to some extent have been influenced similarly to the direction of circulation. However, the main characteristics are believed to be correct.

These are apparently the first experimental results for the effect on natural convection of a partial baffle normal to the isothermal surfaces. A finite-difference solution for the same behavior is presented in a companion paper [13].

Although the results are for glycerol and a $2 \times 1 \times 1$ enclosure they are expected to be applicable qualitatively for air in an enclosure with large aspect ratios.

References

- [1] Chao, P. K.-B., Ozoe, H., and Churchill, S.W., The Effect of a Non-Uniform Surface Temperature on Laminar Natural Convection in a Rectangular Enclosure, *Chem. Eng. Commun.*, vol. 9, pp. 245-254, 1981.
- [2] Chao, P. K.-B., Ozoe, H., Churchill, S.W., and Lior, N., Laminar Natural Convection in an Inclined Rectangular Box with the Lower Surface Half-Heated and Half-Insulated, *J. Heat Transfer*, vol. 105, pp. 425-432, 1983.
- [3] Cane, R.L.D., Hollands, K.G.T., Raithby, G.D., and Unny, T.E., Free Convection in Heat Transfer Across Inclined Honeycomb Panels, *J. Heat Transfer*, vol. 99C, pp. 86-91, 1977.
- [4] Arnold, J.N., Edwards, D.K., and Catton, I., Effect of Tilt and Horizontal Aspect Ratio on Natural Convection in a Rectangular Honeycomb, *J. Heat Transfer*, vol. 99C, pp. 120-122, 1977.
- [5] Emery, A.F., Exploratory Studies of Free-Convection Heat Transfer Through an Enclosed Vertical Layer with a Vertical Baffle, *J. Heat Transfer*, vol. 91C, pp. 163-165, 1969.
- [6] Probert, S.D., and Ward, J., Improvements on the Thermal Resistance of Vertical Air-Filled Enclosed Cavities, *Proc. 5th Int. Heat Transfer Conf., Tokyo*, NC3.9, pp. 124-128, 1974.
- [7] Janikowski, H.E., Ward, J., and Probert, S.D., Free Convection in Vertical, Air-Filled Rectangular Cavities Fitted with Baffles, *Proc. 6th Int. Heat Transfer Conf., Toronto*, vol. 2, pp. 257-262, Hemisphere Publishing, Washington, D.C., 1978.
- [8] Nansteel, M.W., and Greif, R., Natural Convection in Undivided and Partially Divided Rectangular Enclosures, *J. Heat Transfer*, vol. 103C, pp. 623-629, 1981.
- [9] Bauman, F., Gadgil, A., Kammerud, R., and Greif, R., Buoyancy-Driven Convection in Rectangular Enclosures: Experimental Results and Numerical Calculations, *19th National Heat Transfer Conf.*, Orlando, ASME Paper 80-HT-66, 1980.
- [10] Chang, L.C., Yang, K.T., and Lloyd, J.R., Radiation-Natural Convection Interactions in Two-Dimensional Complex Enclosures, *AIAA/ASME 3rd Joint Thermophysics, Fluids, Plasma & Heat Transfer Conference*, St. Louis, Paper 82-HT-49.
- [11] Winters, K.H., The Effect of Conducting Divisions on the Natural Convection of Air in a Rectangular Cavity with Heated Side Walls, *AIAA/ASME 3rd Joint Thermophysics, Fluids, Plasma & Heat Transfer Conference*, St. Louis, Paper 82-HT-69.
- [12] Duxbury, D., An Interferometric Study of Natural Convection in Enclosed Plane Air Layers with Complete and Partial Central Vertical Divisions, Ph.D. Thesis, University of Salford, U.K., 1981.
- [13] Chao, P. K.-B., Ozoe, H., Churchill, S.W., and Lior, N., The Effect of Partial Baffles on Natural Convection in an Inclined Rectangular Enclosure, Part II. Finite-Difference Calculations, *Chem. Eng. Fundam.*, in this paper.
- [14] Newman, A.A., *Glycerol*, Neill & Co., Ltd., Edinburgh, 1968.
- [15] Ozoe, H., Sato, N., and Churchill, S.W., Experimental Confirmation of the Three-Dimensional Helical Streaklines Previously Computed for Natural Convection in Inclined Rectangular Enclosures, *Kagaku Kogaku Ronbunshu*, vol. 5, pp. 19-25, 1979; English transl. *Int. Chem. Eng.*, vol. 19, pp. 454-462, 1979.

Acknowledgement

This work was supported in part by the U.S. Department of Energy Solar Heating and Cooling R + D Branch through Contract EM-78-04-5365, and in part by Special Research Projects on Energy Problems of Grants-in-Aid for Scientific Research, Ministry of Education, Japan (No. 57040075). The participation of Prof. Ozoe in the work at the University of Pennsylvania was cosponsored by the Japan Society for the Promotion of Science and the U.S. National Science Foundation.